Supporting Information

Direct Evidence of Photoinduced Charge Transport Mechanism in 2D Conductive Metal Organic Frameworks

James Nyakuchena,[a] Sarah Ostresh,[b] Daniel Streater,[a] Brian Pattengale,[b] Jens Neu,[c] Christian Fiankor,[c] Wenhui Hu,[a] Eli Diego Kinigstein,[e] Jian Zhang,[d] Xiaoyi Zhang,[e] Charles A. Schmuttenmaer,[b] Jier Huang*[a]

[a]Department of Chemistry, Marquette University, Milwaukee, 53201, United States

[b]Department of Chemistry and Yale Energy Science Institute, Yale University, New Haven, Connecticut, 06520, United States

[c]Department of Molecular Biophysics and Biochemistry and Yale Microbial Sciences Institute, Yale University, New Haven, Connecticut 06520-8107, Unites States

[d]Department of Chemistry, University of Nebraska-Lincoln, Lincoln, Nebraska, 68588

[e]X-ray Science Division, Argonne National Laboratory, Argonne, Illinois, 60349

Corresponding Author

* Jier Huang (jier.huang@marquette.edu)

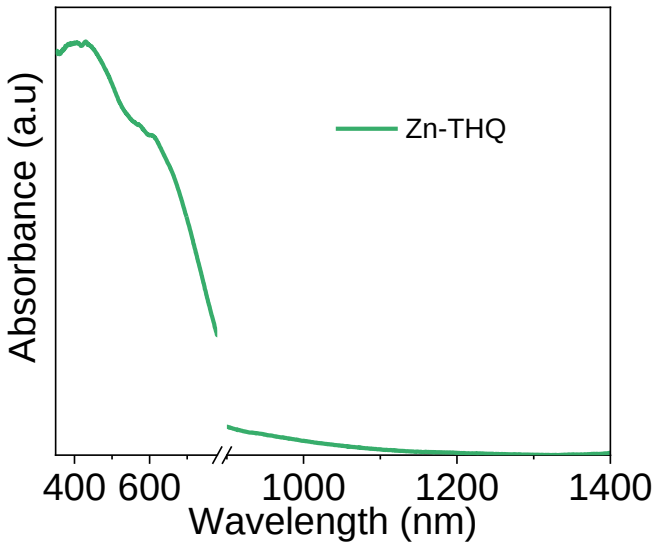

Figure S1. a) The diffuse reflectance UV-visible-near IR spectrum of Zn-THQ MOF.

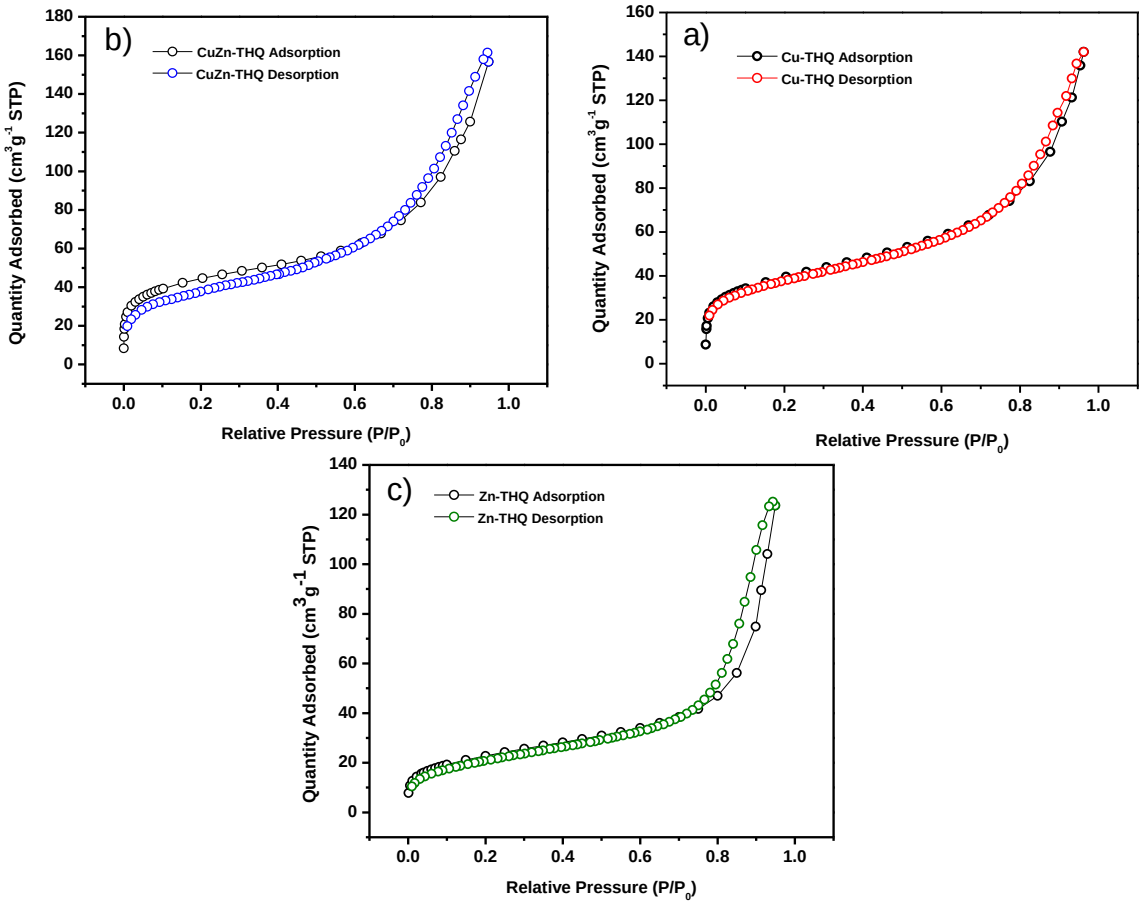

Figure S2. a) N_2 sorption isotherms at 77 K for Cu-THQ a), Cu/Zn-THQ (b), and Zn-THQ (c).

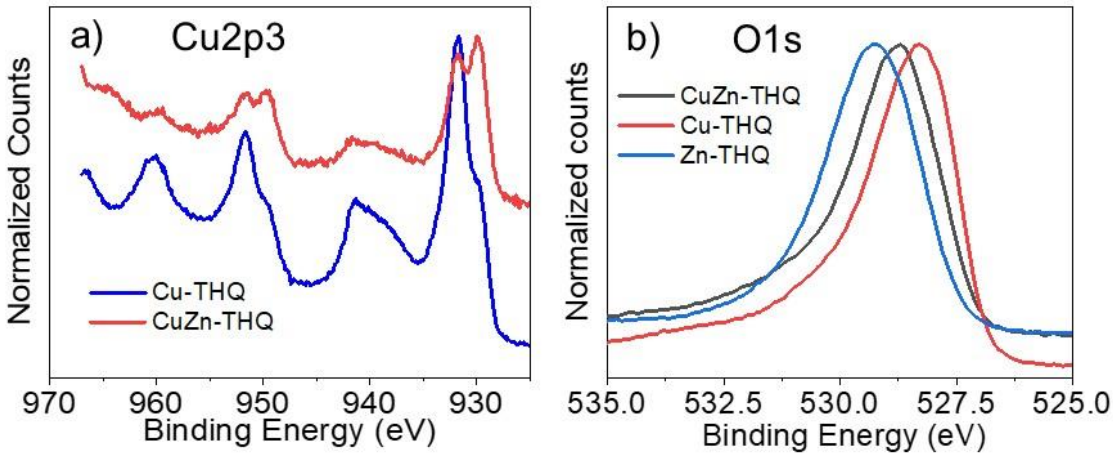

Figure S3. XPS spectra for THQ MOFs a) Binding energy comparison for a) Cu2p3 and b) O 1s

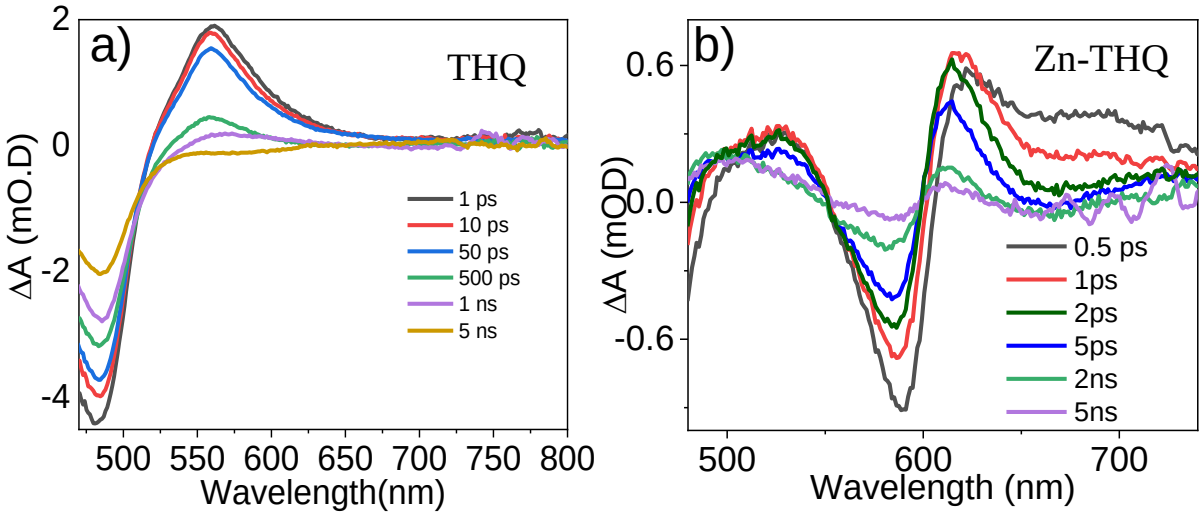

Figure S4. OTA spectra of THQ ligand in chloroform solution (a) and Zn-THQ following 450 nm excitation.

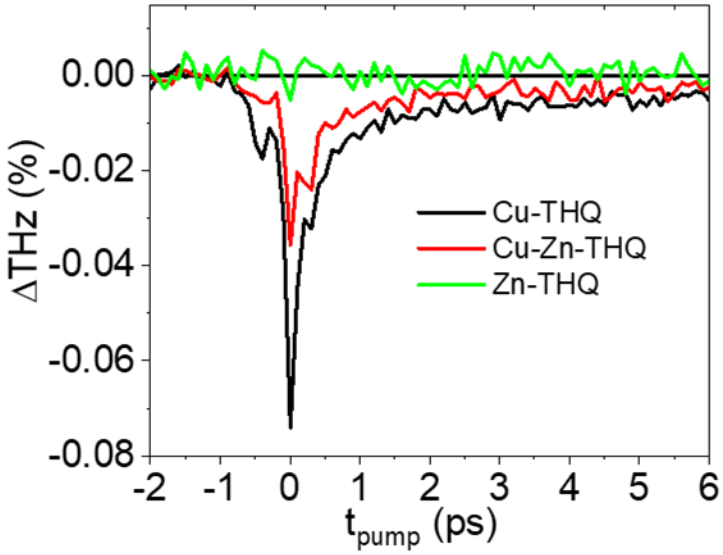

Figure S5. Normalized OPTP traces for all three MOF samples. The solid black baseline indicates that the signal does not return to baseline within the measured time range of 300 ps.

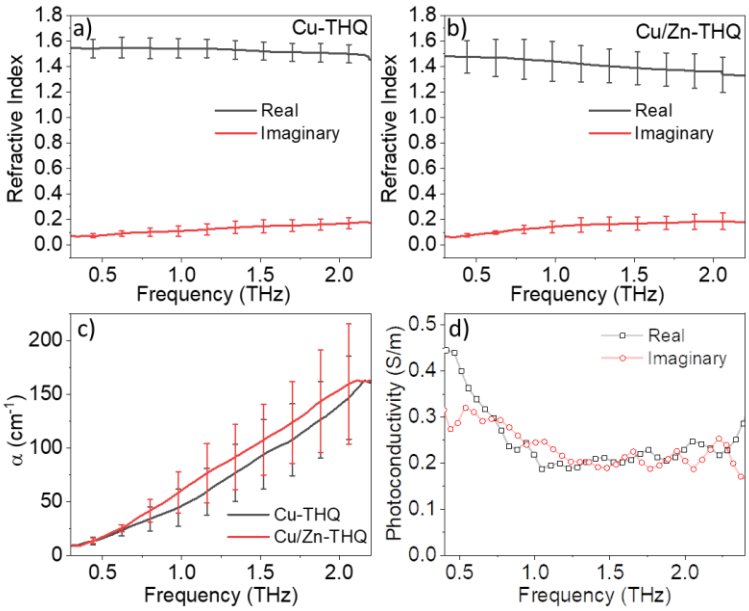

Figure S6. Time-domain THz spectroscopy (THz-TDS) for Cu-THQ (a) and Cu/Zn-THQ (b). Comparison of the absorption coefficient α (c). Frequency-dependent photoconductivity spectrum of Cu-THQ (d). The photoconductivity is estimated to be about 0.2 S/m using the relatively flat photoconductivity signal observed between 1 – 2.2 THz.

Table S1. Fitting parameters for OTA kinetic traces of exciton bleach in Cu-THQ and Cu/Zn-THQ.

MOF	τ_1 (ps)	A_1 (%)	τ_2 (ps)	A_2 (%)	τ_3 (ns)	A_3 (%)
Cu-THQ	0.4	75.4	8.2	19.4	>> 5ns	5.2
Cu/Zn-THQ	0.4	77.0	17.0	14.4	>> 5ns	8.6

Table S2. Table of fit parameters that describe the dynamics of the decay in the X.T.A traces.

	τ_1 (ns)	A_1 (%)	τ_2 (ns)	A_2 (%)
Cu-THQ	0.6	67.0	33.6	33.0
Cu/Zn-THQ	1.2	50.0	42.4	50.0

Table S3. Table of fit parameters that describe the dynamics of the decay in the OPTP traces.

	τ_1 (ps)	A_1	τ_2 (ps)	A_2	τ_3 (ps)	A_3
Cu-THQ	0.4	0.060	5.65	0.00735	1000	0.00310
Cu-Zn-THQ	0.4	0.035	5.24	0.00351	1000	0.00198

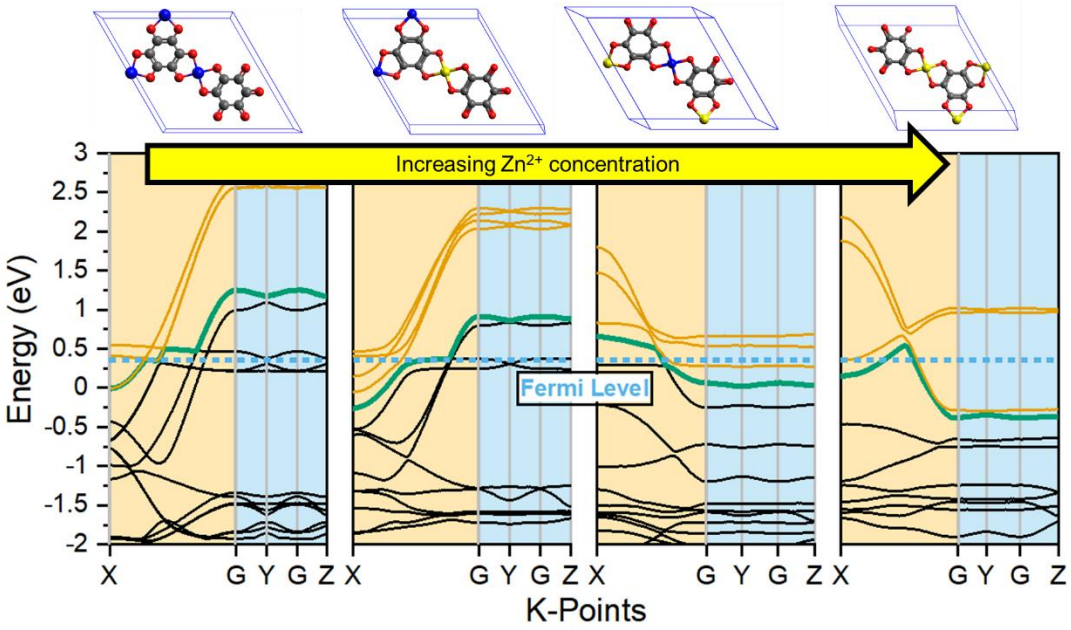

Figure S7. Band structure calculations performed on triclinic unit cells of Cu-THQ with increasing concentration of Zn^{2+} ions (left to right). Axes aligned to show the effect of Zn^{2+} incorporation on Fermi level crossings.

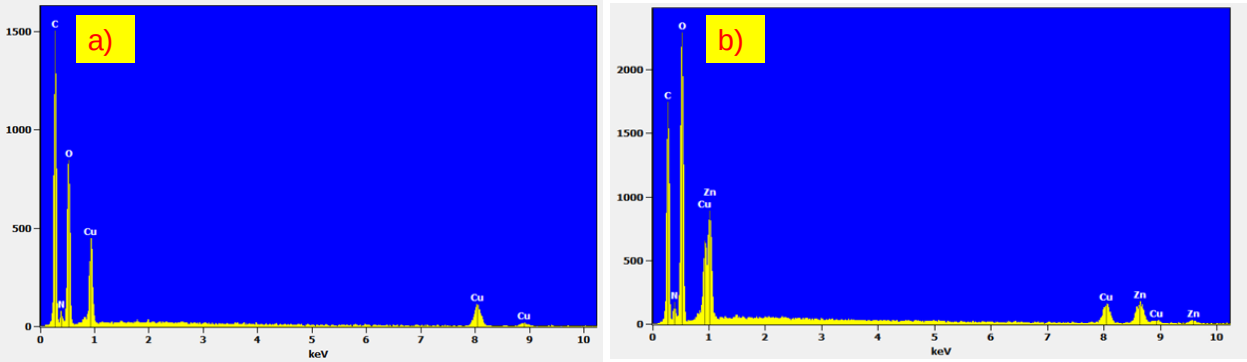

Figure S8. EDX spectra showing elemental composition for Cu-THQ (a) and Cu/Zn-THQ (b). The atomic ratio of Cu to Zn is 44:56.

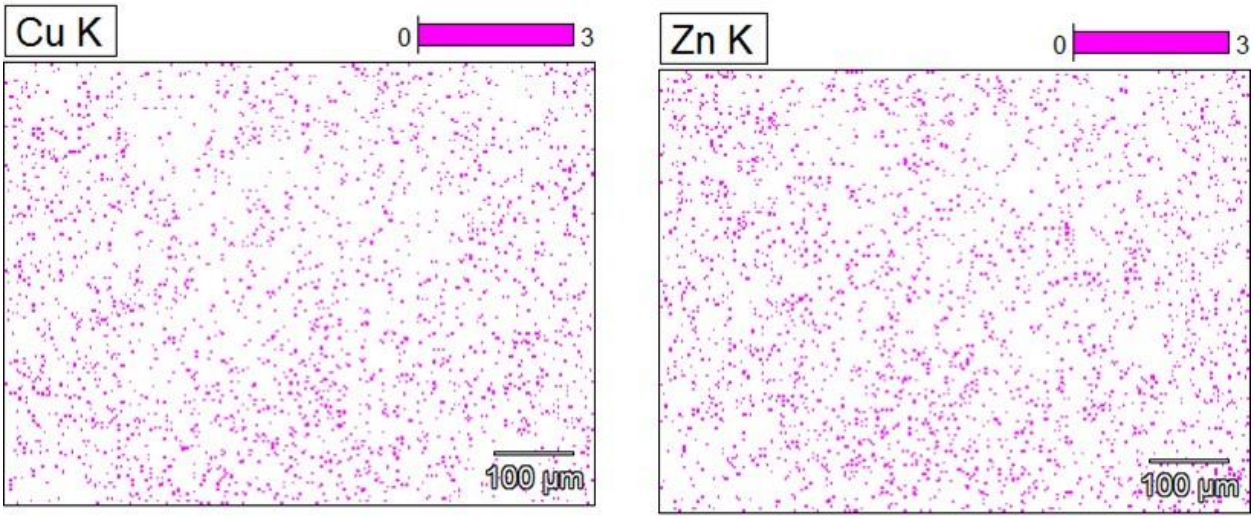

Figure S9. EDX spectra showing elemental distribution for Cu (a) and Zn-THQ (b) in Cu/Zn-THQ

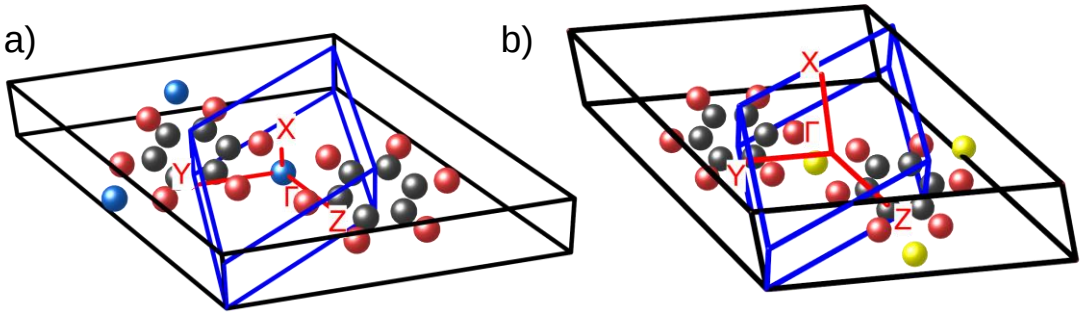

Figure S10. Cu-THQ and Zn-THQ unit cells with atomic positions and the real-space interpretation of the Brillouin zone.